

Supporting Information

Endothelial Dysfunction and Transcriptome Aberration in Mouse Aortas Induced by Black Phosphorus Quantum Dots and Nanosheets

Jiayan Chen,^a Liping Lu,^a Chunlong Zhang,^b Xiaoming Zhu,^c and Shulin Zhuang*^a

^a Key Laboratory of Environment Remediation and Ecological Health, Ministry of Education, College of Environmental and Resource Sciences, Zhejiang University, Hangzhou 310058, China

^b Department of Environmental Sciences, University of Houston-Clear Lake, 2700 Bay Area Blvd., Houston, Texas 77058, USA

^c Key Laboratory of Women's Reproductive Health Research of Zhejiang Province, Women's Hospital, School of Medicine, Zhejiang University, Hangzhou 310006, China

* corresponding author: shulin@zju.edu.cn (S. Z.)

A total of 11 pages including 2 tables and 8 figures

Table S1. The primers used for qPCR.

Gene	Primer Sequences (5' to 3')
Human eNOS	CCGAGTCCTCACCGCCTTCT GGTAACATCGCCGCAGACAAA
Human iNOS	CCGAGGCAAACAGCACATTGAGAT GAGTCCTGCACGAGCCTGTA
Human GAPDH	CCATGACAACCTTTGGTATCGTGGAA GGCCATCACGCCACAGTTTC
Mouse Myl4	ACATCTCCCGCAACAAGG TCTCCCAGGGTAGCAAGG
Mouse Myh6	GCAGGACCTGGTGGACAA ACCTTGCGGAACTTGGAC
Mouse Tnnc1	TGACAGAGGAGCAGAAGAA TGTAGCCATCAGCGTTTT
Mouse GAPDH	CCTTCCGTGTTCTACCC CAACCTGGTCCTCAGTGTAG

Table S2. The total DEGs and the number of upregulated or downregulated DEGs in aortas of mice after exposure to BP on day 1 and day 7 (BPQD_1 and BPNS_1 refer to 1 day after exposure to BP; BPQD_7 and BPNS_7 refer to 7 days after exposure to BP).

Treatment	Number of DEGs	Upregulation	Downregulation
BPQD_1	974	781	193
BPNS_1	1399	1141	258
BPQD_7	1155	475	680
BPNS_7	1702	1291	411

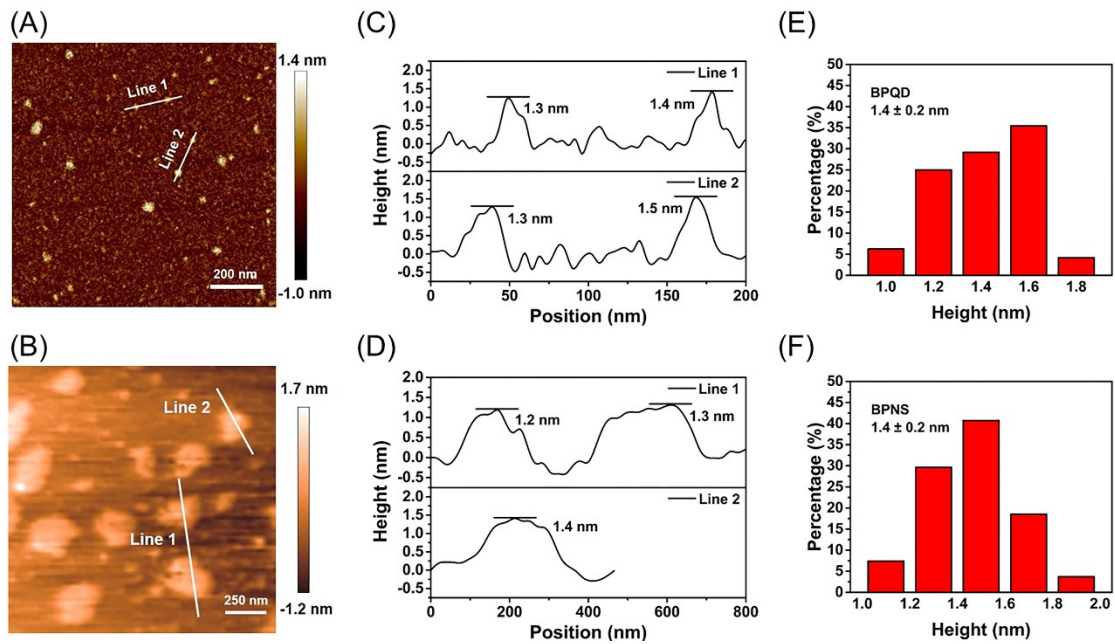
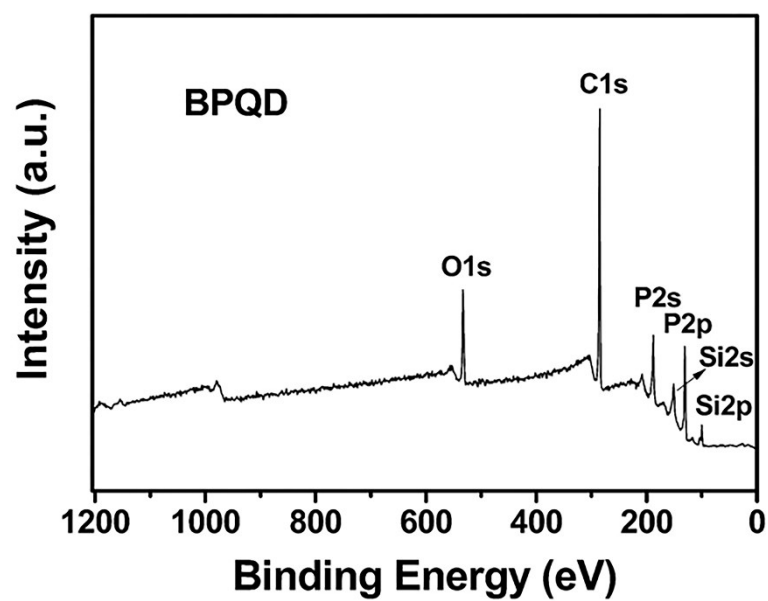


Figure S1. AFM characterization of BPQDs and BPNSs. Representative AFM topography of BPQDs (A) and BPNSs (B). (C) and (D) are height profiles along the white lines in (A) and (B), respectively. Statistical analysis of the heights of BPQDs (E) and BPNSs (F).

(A)



(B)

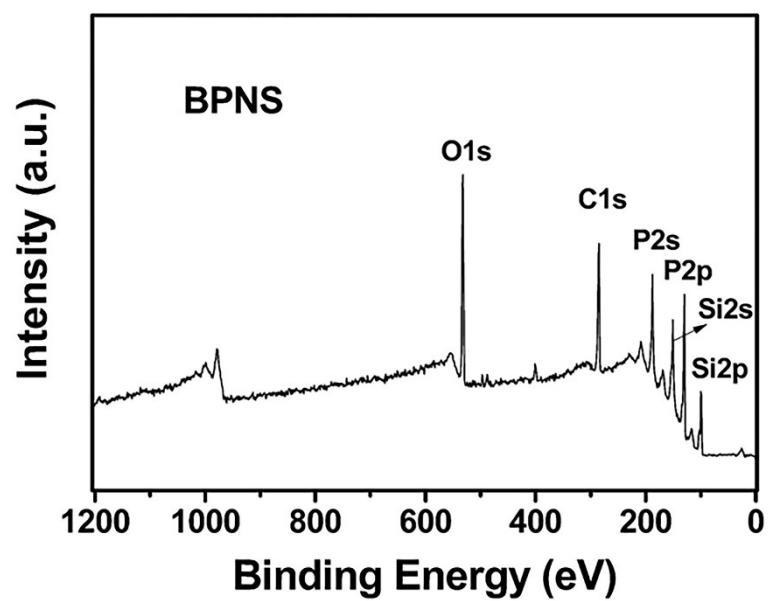


Figure S2. XPS spectra of BPQDs (A) and BPNSs (B).

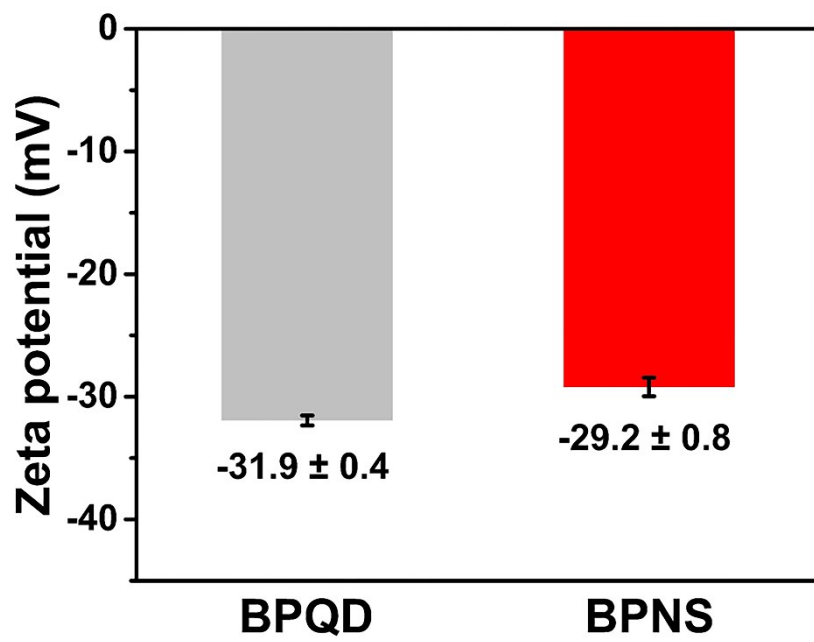


Figure S3. Zeta potential of BPQDs and BPNSs.

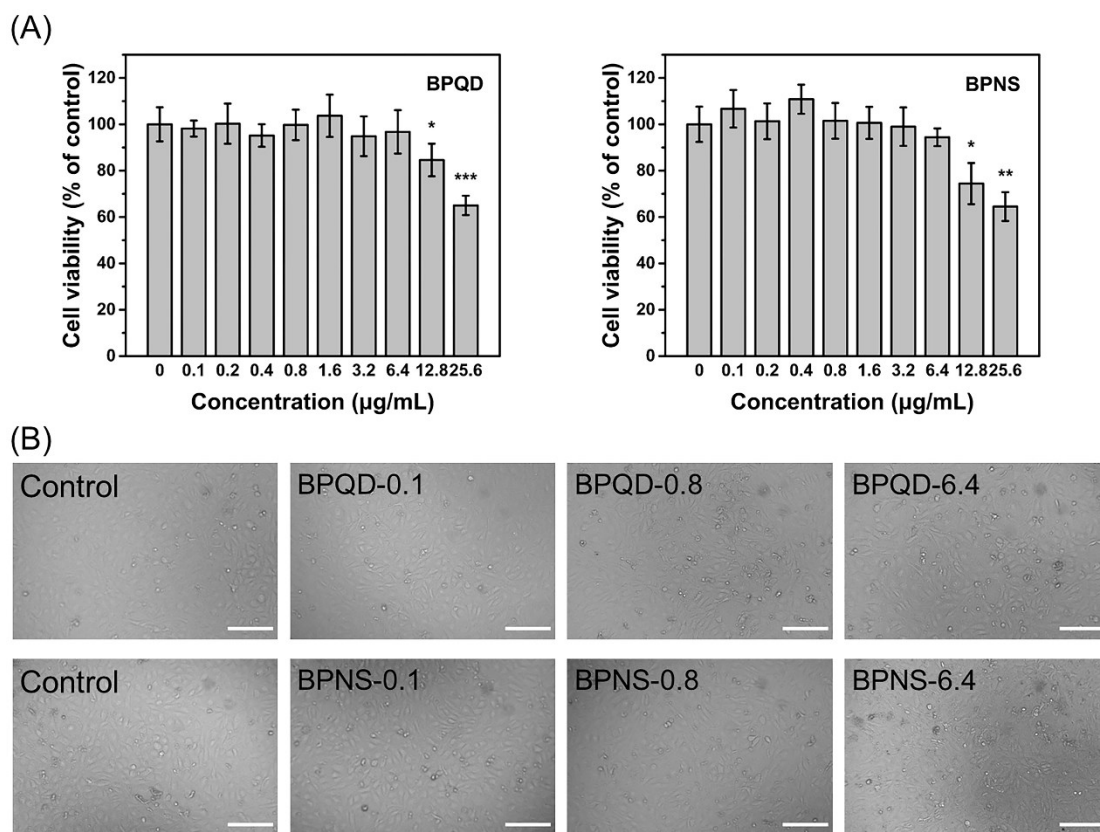


Figure S4. (A) Cell viability of HUVECs after 24 h incubation with BPQDs and BPNSs at different concentrations ranging from 0 to 25.6 µg/mL. (B) Representative optical microscopy images of HUVECs after 24 h incubation with BPQDs and BPNSs at 0.1, 0.8 and 6.4 µg/mL (Scale bar: 200 µm).

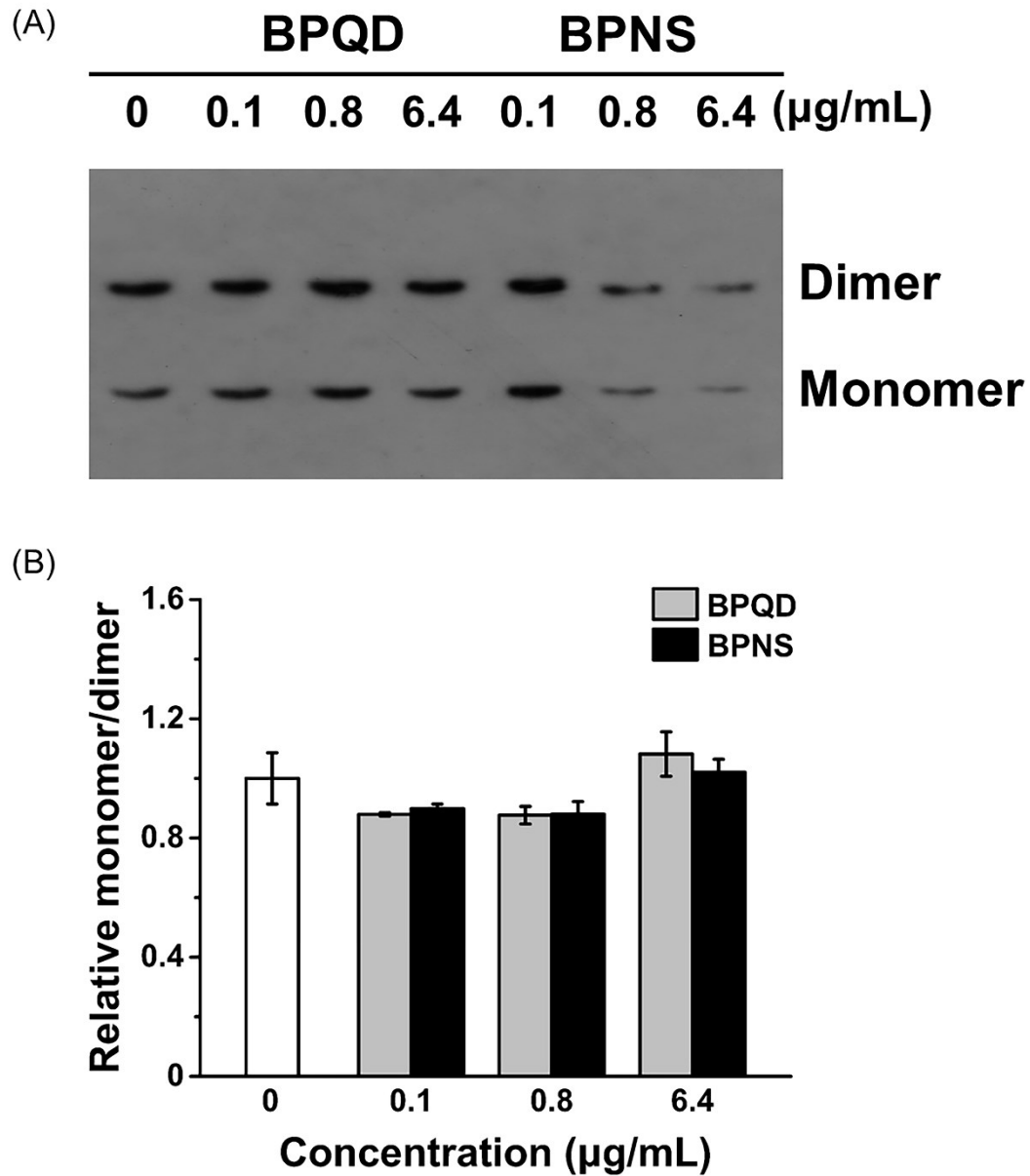


Figure S5. HUVECs were treated with BPQDs or BPNSs at the concentrations of 0.1, 0.8 and 6.4 $\mu\text{g/mL}$ for 24 h. (A) Dimeric and monomeric form of eNOS determined by western blot. (B) The relative ratio of monomer to dimer of eNOS. Data shown represent mean fold change (\pm SD) relative to untreated cell.

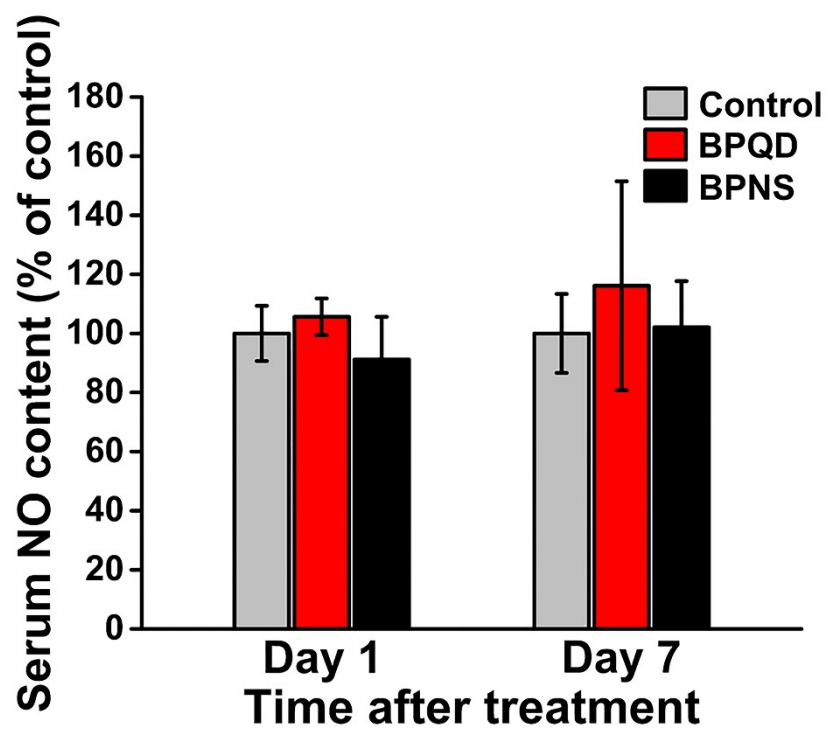


Figure S6. Serum NO level in mice intravenously injected with the BPQDs and BPNSs at 1 and 7 days post-administration.

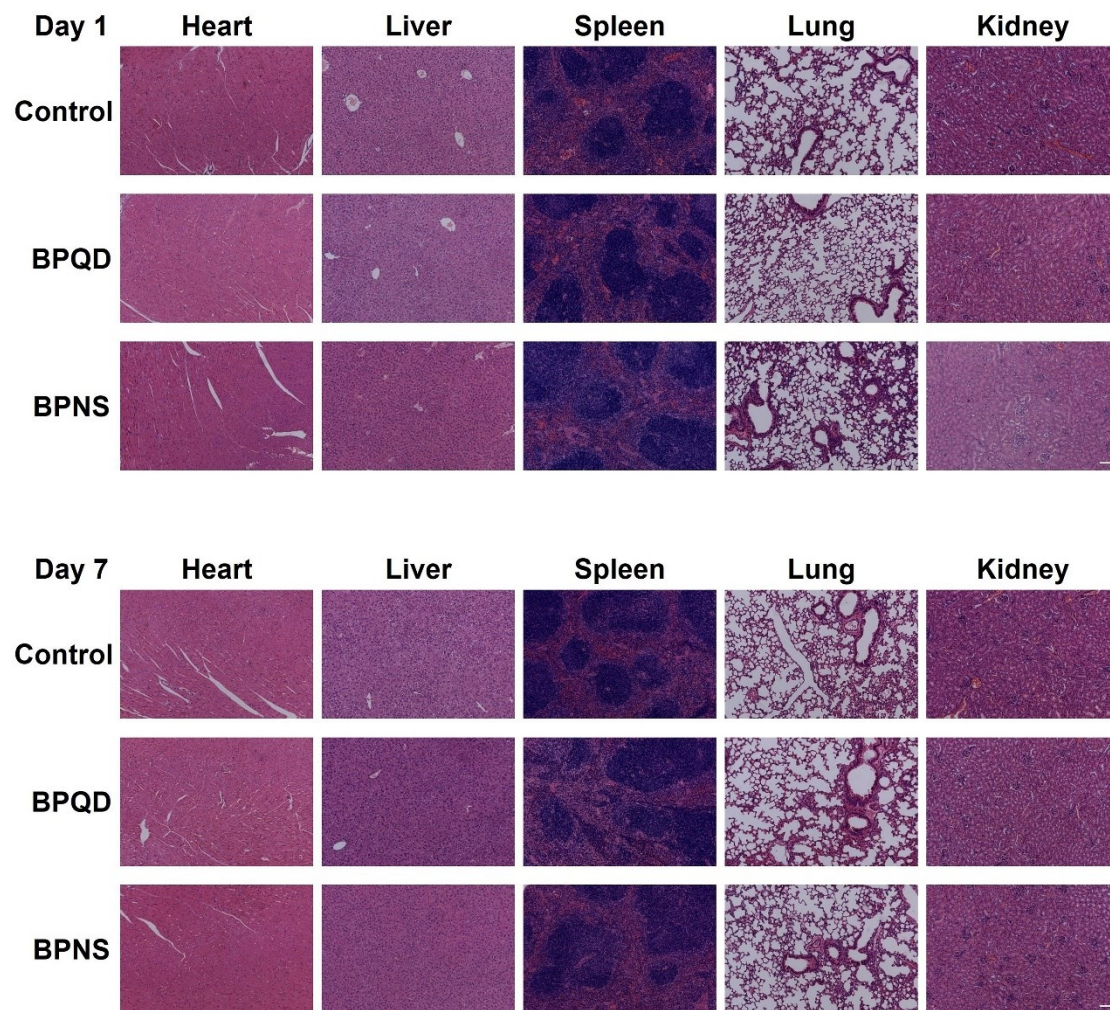


Figure S7. Histopathology evaluation following hematoxylin and eosin staining of heart, liver, spleen, lung, and kidney (Scale bar: 100 μ m).

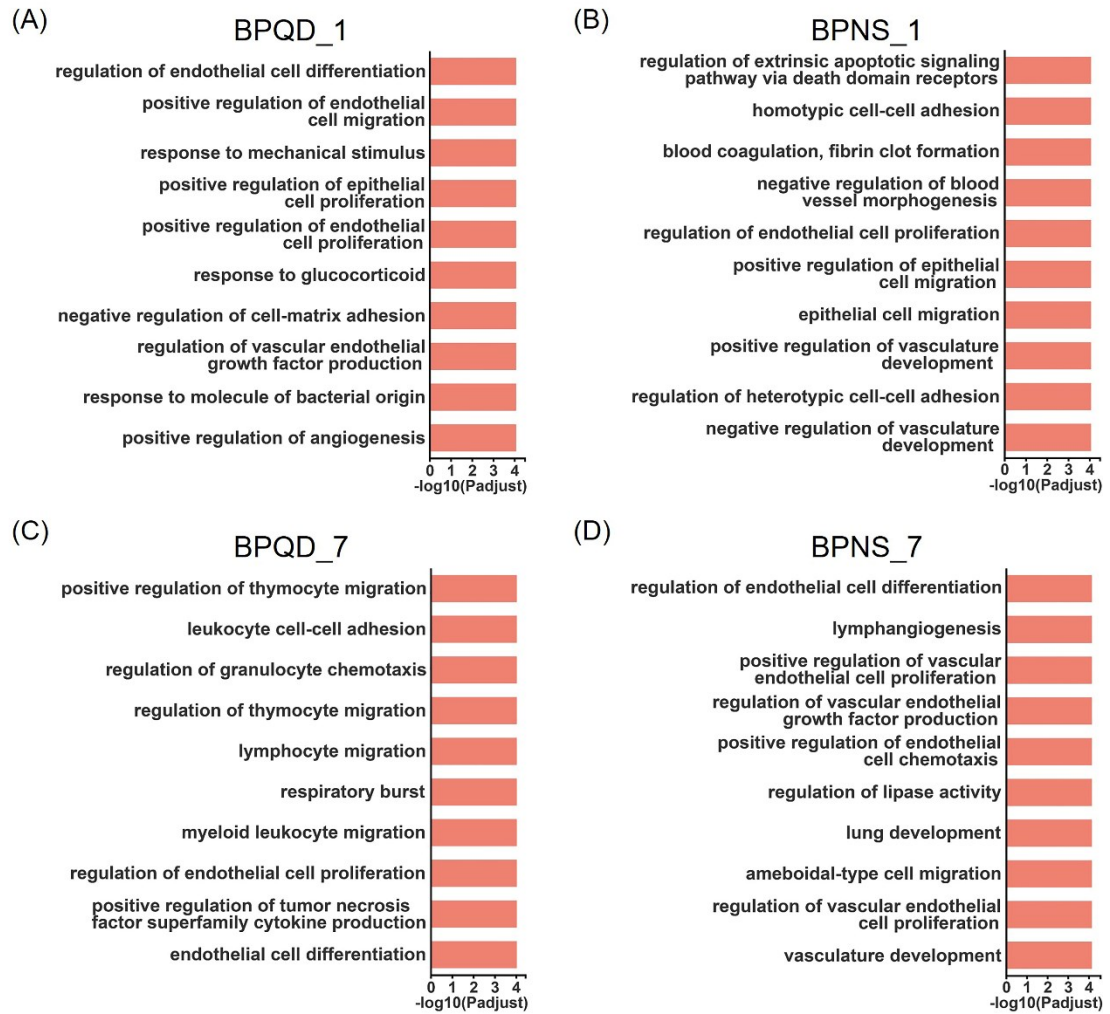


Figure S8. GO enrichment analysis of the endothelial-related DEGs affected by BPQDs (A) or BPNSs (B) 1 day after administration, and by BPQDs (C) or BPNSs (D) 7 days after administration.